

Mueller-matrix characterization of liquid crystals

J.N. Hilfiker^{a,*}, C.M. Herzinger^a, T. Wagner^b, Antigone Marino^c, Guisepe Delgais^c, Giancarlo Abbate^c

^aJ.A. Woollam Co., Inc., 645 M Street, Suite 102, Lincoln, NE 68508, USA

^bL.O.T.-Oriet GmbH, Im Tiefen See 58, Darmstadt 64293, Germany

^cINFN and Università di Napoli Federico II, Via Cintia Monte S. Angelo, I-80126 Napoli, Italy

Abstract

Generalized spectroscopic ellipsometry (g-SE) has been applied to many anisotropic materials. This measurement is based on the 2×2 Jones matrix sample representation, which is often sufficient. However, when the reflected or transmitted light becomes sufficiently depolarized, the Mueller-matrix (MM) representation may be required for anisotropic materials characterization. We report measurements of a $33.85 \mu\text{m}$ thick liquid crystal layer sandwiched between two glass substrates. In addition to the sample anisotropy, the measurement is significantly depolarized. Mueller-matrix measurements are acquired in transmission as a function of wavelength, angle of incidence, and sample orientation to characterize the liquid crystal layer. Experimental measurements allow characterization of the liquid crystal anisotropy and orientation.

© 2004 Elsevier B.V. All rights reserved.

Keywords: Mueller matrix; Generalized ellipsometry; Liquid crystals; Anisotropy

1. Introduction

Anisotropic liquid crystal layers have been studied with generalized ellipsometry [1–3]. This measurement is based on the 2×2 Jones matrix including both diagonal and off-diagonal elements. This representation is often sufficient for characterizing anisotropic materials.

However, the Jones matrix assumes the measurement light remains polarized. When the reflected or transmitted light becomes partially polarized, it may be necessary to incorporate the MM representation.

The MM maps changes in Stokes parameters for the measurement beam, as [4]:

$$\begin{bmatrix} S_0 \\ S_1 \\ S_2 \\ S_3 \end{bmatrix}_{\text{OUT}} = \begin{bmatrix} M_{11} & M_{12} & M_{13} & M_{14} \\ M_{21} & M_{22} & M_{23} & M_{24} \\ M_{31} & M_{32} & M_{33} & M_{34} \\ M_{41} & M_{42} & M_{43} & M_{44} \end{bmatrix} \cdot \begin{bmatrix} S_0 \\ S_1 \\ S_2 \\ S_3 \end{bmatrix}_{\text{IN}} \quad (1)$$

For certain classes of samples this matrix contains symmetries, so it is not necessary to independently measure all 16 parameters for most materials characterization. For example, the MM of an isotropic sample remains block diagonal and is given by [4]:

$$\begin{bmatrix} 1 & -N & 0 & 0 \\ -N & 1 & 0 & 0 \\ 0 & 0 & C & S \\ 0 & 0 & -S & C \end{bmatrix} \quad (2)$$

where $N = \cos(2\Psi)$, $C = \sin(2\Psi)\cos(\Delta)$, and $S = \sin(2\Psi)\sin(\Delta)$. The MM also remains block diagonal for anisotropic materials when the optical axes are oriented parallel or perpendicular to the plane of incidence. For example, the MM of an ideal retarder with phase shift, δ , is [5]:

$$\begin{bmatrix} 1 & 0 & 0 & 0 \\ 0 & 1 & 0 & 0 \\ 0 & 0 & \cos(\delta) & -\sin(\delta) \\ 0 & 0 & \sin(\delta) & \cos(\delta) \end{bmatrix} \quad (3)$$

*Corresponding author. Tel.: +1-402-477-7501x127; fax: 1-402-477-8214.

However, the block off-diagonal MM elements will not remain zero for other anisotropy orientations. For example, the MM for a retarder that is rotated by θ from the ellipsometer coordinate system, is given by [5]:

$$\begin{bmatrix} 1 & 0 & 0 & 0 \\ 0 & \cos^2(2\theta) + \cos(\delta)\sin^2(2\theta) & (1 - \cos(\delta))\sin(2\theta)\cos(2\theta) & \sin(\delta)\sin(2\theta) \\ 0 & (1 - \cos(\delta))\sin(2\theta)\cos(2\theta) & \sin^2(2\theta) + \cos(\delta)\cos^2(2\theta) & -\sin(\delta)\cos(2\theta) \\ 0 & -\sin(\delta)\sin(2\theta) & \sin(\delta)\cos(2\theta) & \cos(\delta) \end{bmatrix} \quad (4)$$

The MM remains valid when the measurement becomes partially polarized. For this reason MM measurements can be applied to samples that are both anisotropic and depolarizing.

In this study, we use MM transmission measurements to characterize a thick liquid crystal layer. The LC film (Merck ZLI 3700) is sandwiched between glass substrates with 30 μm spacers. Each substrate is coated with a thin polyimide alignment layer that was spin-coated, cured at 300 $^\circ\text{C}$ for 2 h, and then rubbed to orient the surface. The LC layer is estimated to be 33.85 μm thick, which corresponds to spectrophotometer measurements of the empty cell gap prior to filling with LC material.

2. Measurement

To characterize liquid crystals, it is beneficial to measure the transmitted light as a function of wavelength and angle of incidence. Transmission measurements reduce the amount of unwanted incoherent light reaching the detector as a result of interference within the thick substrate layers [6].

Reported measurements were taken with a rotating analyzer ellipsometer (RAE) that incorporates an adjustable compensator prior to the sample [7]. With a retarder before the sample, all four Stokes parameters can be controlled (INPUT light in Eq. (1)). However, only the S_0 , S_1 , and S_2 parameters can be detected at the OUTPUT because there is no retarder in the RAE detection configuration. Thus, measurements are sensitive to the first three rows of the MM and completely insensitive to the bottom row. Each of the measured values is normalized to the M_{11} element.

For the first three rows, the MM for a sample described by a non-depolarizing Jones matrix can be extracted [8]. Furthermore, for certain standard sources of depolarization (thickness non-uniformity, angle spread, finite optical bandwidth), the resulting MM is due to a smearing of polarization state over a range of similar Jones matrices, which still allow the sample to be characterized by a physical model using only the first three rows of MM elements.

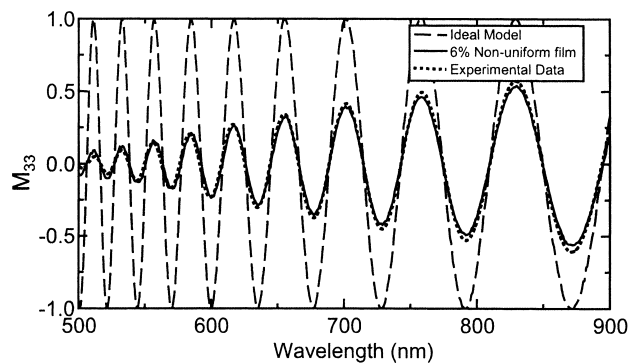


Fig. 1. Experimental M_{33} data graphed along with curves from an ideal model and a model incorporating 6% thickness non-uniformity. The non-uniform thickness produces the depolarization needed to suppress oscillation amplitudes to match the experimental curve.

The eleven MM elements are measured as a function of wavelength, angle of incidence, and sample orientation to characterize the liquid crystal layer. This provides a large amount of data that can be simultaneously analyzed to determine the liquid crystal anisotropy and orientation.

3. Results and discussion

Measurements assuming a Jones matrix form for the sample were unsuccessful because the Jones matrix does not adequately represent the sample. Instead, MM measurements were used to characterize this sample. The data analysis show significant influence due to depolarization on each of the oscillating MM elements. Fig. 1 illustrates the effects of depolarization from measurements with a 2 mm beam diameter and 2 nm wavelength bandwidth on the measured M_{33} element at normal incidence in transmission. The data oscillations are due to interference between the ordinary and extraordinary rays. The predicted M_{33} result for polarized light has the same oscillating frequency (due to anisotropy), but without damping. To predict the amplitude suppression toward shorter wavelengths requires inclusion of a depolarizing effect in the model. Depolarization can come from incoherent multiple reflections within thick substrates, lateral non-uniform film properties, angular spread, patterned surfaces, and finite wavelength bandwidth. The measurement shown in Fig. 1 may include multiple depolarizing effects. The model used in Fig. 1 to match the experimental curve considers only 6% thickness non-uniformity, demonstrating the high sensitivity of data to lateral film uniformity.

Further measurements demonstrate the true sources of depolarization. These experiments provide more accurate modeling and suggest methods to eliminate the depolarization. Without significant depolarization, Jones measurements may again be adequate to characterize this

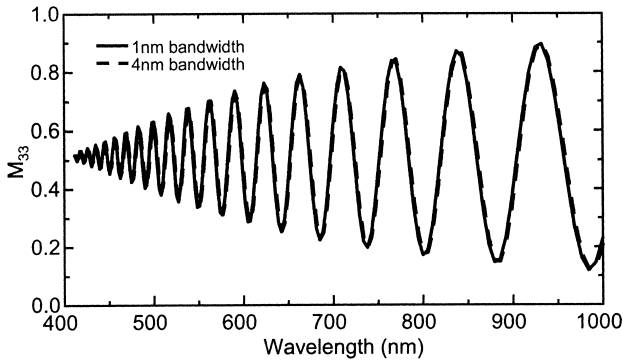


Fig. 2. Comparison of two experimental M_{33} curves with constant measurement conditions except instrument bandwidth, which was fixed to 1 and 4 nm for consecutive measurements.

material. The two measurements compared in Fig. 2 were taken with measurement optical bandwidth of 1 and 4 nm while all other measurement conditions remained constant. The similarity of the two data sets suggests the optical bandwidth is not contributing significantly to depolarization.

Fig. 3 compares measurements with 1 and 4 mm spot size, while all other conditions are fixed. The data oscillations are significantly suppressed for the 4 mm beam diameter, as compared to the data from the 1 mm beam diameter. This suggests an increase in film depolarization as the spot size increases, and concludes that this is the major source of depolarization. The sample dimensions were small (1 by 1 cm) and the film was more uniform in the center. As the beam size gets larger, it collects data from the non-uniform outer regions. While depolarization effects are not eliminated with the smaller beam diameter, they are reduced. To further minimize depolarization with the goal of characterizing this sample with g-SE, the measurement could be taken at longer wavelengths (where non-uniform thickness produces a lower percentage of depolarization) or with a smaller spot size. However, if the beam is focused, angular spread can introduce another possible source of depolarization. Thus, we chose to characterize the sample with MM transmission measurements using a collimated light beam irised to 2 mm diameter. The sample was aligned such that the LC process direction was in the ellipsometer plane of incidence. The MM is block-diagonal and takes the form of Eq. (3) when the optical axis is aligned with the ellipsometer. As the sample is rotated, the MM takes the form of Eq. (4) with information in the off-block diagonal elements (M_{23} , M_{24} , and M_{32}). At normal incidence, the M_{12} and M_{21} elements will be zero because $\Psi = 45^\circ$. Measurements of the transmitted MM at normal incidence measurements were acquired as a function of sample rotation, θ , which moves the x - and y -orientations away from the p - and s -ellipsometer directions, respectively. In general, a

dense set of sample rotations is not necessary but this helps demonstrate the correct model is used. Fig. 4 shows how the MM changes from the form of Eq. (3) to that of Eq. (4) as the sample orientation is rotated to move the optical axis away from the p -plane. Although all eleven measured MM elements are included in data analysis. Fig. 5 presents the non-zero MM curves. In each figure, the MM measurements are graphed along with corresponding model for multiple sample orientations. The good agreement of this model for both incident angle and sample rotation insures the correct sample description.

The spectroscopic MM measurements at normal incidence are included in a simultaneous fit to angle dependent measurements. The Mueller-matrix measurements as a function of incident angle are shown in Fig. 6. It is evident that the liquid crystal orientation is tilted due to the symmetry shift away from normal incidence (0°) for the MM elements. The eleven measured MM elements are graphed in Fig. 6 for photon energy of 1.5 eV. The model fit curves in this figure determine a 16° z -axis tilt into the plane of incidence.

The final model describes the liquid crystal layer as a biaxial anisotropic layer ($n_x \neq n_y \neq n_z$). Strong anisotropy exists between the x - and y -orientations (which correspond to p - and s -ellipsometer directions), as illustrated in Fig. 6. This anisotropy was described using a 5-term polynomial, as:

$$\Delta\varepsilon = A + \frac{B}{\lambda^2} + \frac{C}{\lambda^2} + \frac{D}{\lambda^2} + E\lambda^2 \quad (5)$$

where all five polynomial parameters (A , B , C , D , and E) were allowed to vary.

Liquid crystal materials are often uniaxial, but the experimental features required a biaxial description of the layer. The z -axis for this model is tilted 16° in the plane of incidence. Anisotropy between the z - and x -orientation is shown in Fig. 7. The index difference

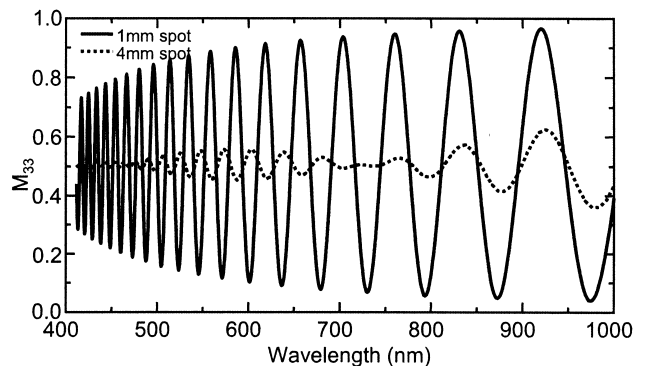


Fig. 3. Comparison of two experimental M_{33} curves with constant measurement conditions except spot size, which was fixed at 1 and 4 mm for consecutive measurements.

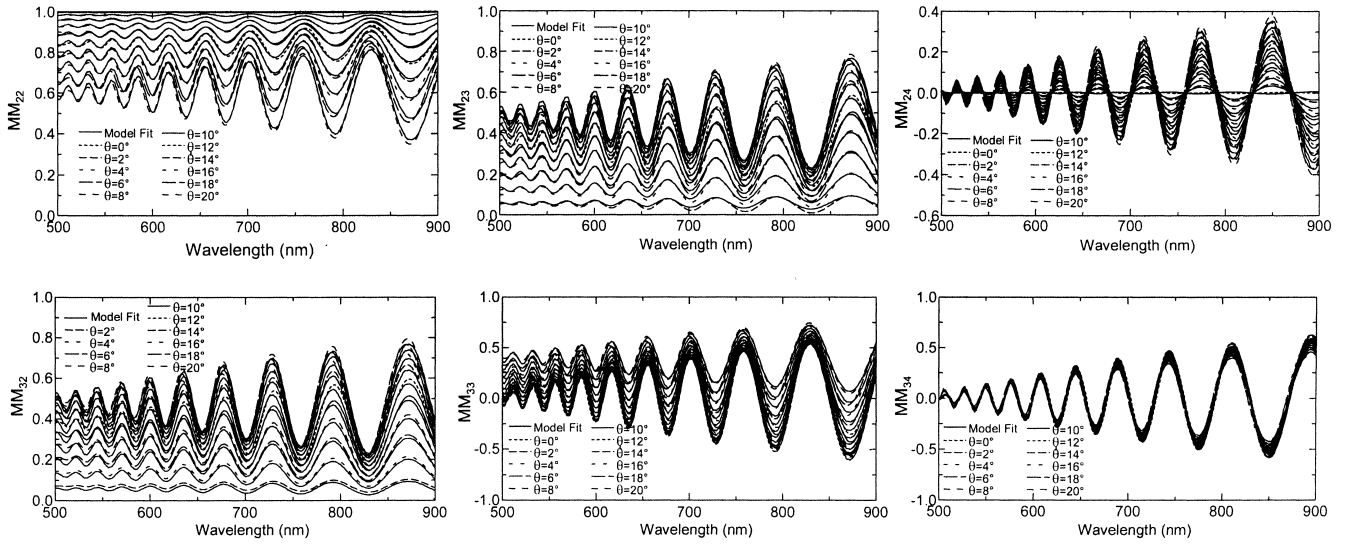


Fig. 4. Spectroscopic MM measurements taken in transmission at normal incidence over a series of sample orientations, along with the corresponding model fit. Although eleven normalized elements were measured and analyzed, the prominent data features are witnessed in the M_{22} , M_{23} , M_{24} , M_{32} , M_{33} , and M_{34} elements shown.

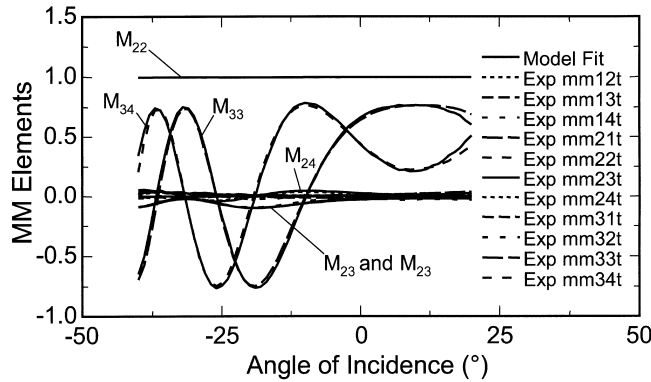


Fig. 5. Experimental MM measurements (eleven normalized elements) at 1.5 eV over a range of incident angles, along with the corresponding fit with a model that tilts the z -axis 16° in the plane of incidence. The shifted symmetry away from normal incidence indicates this tilted orientation.

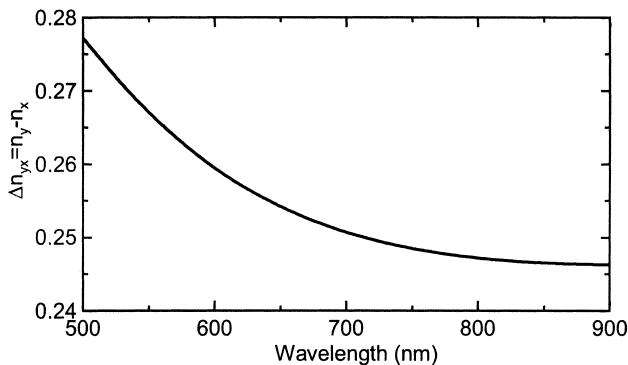


Fig. 6. Anisotropy between the x - and y - liquid crystal orientation.

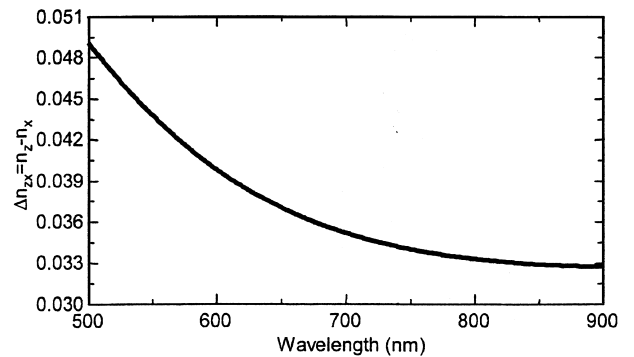


Fig. 7. Anisotropy between the x - and z - liquid crystal orientation. The orientation of the z -axis is tilted by 16° into the plane of incidence.

(anisotropy) was described using a 2-term polynomial with only the A and B parameters of Eq. (5).

Additional features were investigated which allow the liquid crystal orientation to vary with film depth, as is common in commercial displays. However, this model did not improve the fit quality. Accurate index values require information from oblique angles of incidence near to the Brewster condition, which contain a larger Fresnel contribution. The near-normal measurements used for this characterization are very sensitive to anisotropy and orientation, but largely insensitive to the absolute index. The final fit index for the x -orientation was 1.43 with a fixed Sellmeier-dispersion shape, although the accuracy of this measurement is in question without more oblique angle measurements. By avoiding oblique angles, the isotropic films coated on each glass substrate could also be ignored. More complete characterization of the liquid crystal sample would require a better understanding of the complete sample structure and measurements at oblique angles, as performed in a companion paper [8].

The anisotropy measurement provides high sensitivity due to the large path length through the film (33.85 microns). Our model assumes the nominal thickness value as measured via spectrophotometry of the unfilled LC cell gap. Any error in the thickness will also affect the anisotropy, as the ellipsometer is measuring the resulting product of thickness and anisotropy. Optical measurements of the actual LC layer thickness are prohibitive because of significant thickness non-uniformity. No coherent oscillations between front and back LC layer surfaces were witnessed from the measurements in this study (the observed oscillations are due to anisotropy, not Fresnel interference). Thus, the typical measurement approach is to first measure the empty air gap, but the relation between this air-gap measurement and final LC layer thickness will affect the final measurement values.

4. Conclusion

The anisotropy (Δn) and orientation angle of a thick liquid crystal layer were characterized with Mueller-matrix measurements. Mueller-matrix measurements were required for this sample because of the strong depolarization and anisotropy of the liquid crystal layer. Investigations show the depolarization to be primarily from non-uniformity of the liquid crystal thickness. This is taken into consideration during modeling to get agreement with experimental data. The measurements include angle-dependent Mueller-matrix to determine the liquid crystal orientation, which was found to tilt 16° from the sample normal. With the determined orientation, Mueller-matrix measurements at normal incidence were fit to determine the anisotropy in the film. These measurements were also taken at different sample rotation angles to insure the correct model interpretation. Good internal agreement was found with in the experimental data sets; as a function of wavelength, incident angle, and sample rotation angle. Final results show the liquid crystal layer is biaxially anisotropic with its most significant anisotropy between in-plane orientations.

References

- [1] M. Schubert, *Thin Solid Films* 313–314 (1998) 323–332.
- [2] M. Schubert, B. Rheinlander, C. Cramer, H. Schmiedel, J.A. Woollam, C.M. Herzinger, B. Johs, *J. Opt. Soc. Am. A* 13 (9) (1996) 1930–1940.
- [3] C. Benecke, H. Seiberle, M. Schadt, *Jpn. J. Appl. Phys.* 39 (2000) 525–531.
- [4] B. Johs, J.A. Woollam, C.M. Herzinger, J. Hilfiker, R. Synowicki, C.L. Bungay, *SPIE Proc. CR72* (1999) 29–58.
- [5] E. Collett, *Polarized Light: Fundamentals and Applications*, Marcel Dekker, New York, 1992, pp. 75–82.
- [6] J.F. Elman, J. Greener, C.M. Herzinger, B. Johs, *Thin Solid Films* 313–314 (1998) 814–818.
- [7] VASE with AutoRetarder from J.A. Woollam Co., Inc.
- [8] G.E. Jellison, *Thin Solid Films*, 313–314 (1998) pp. 33–39.